Lung (2016) 194:501–509
DOI 10.1007/s00408-016-9909-9

Applications of Magnetic Resonance Imaging of the Thorax in Pleural Diseases: A State-of-the-Art Review

Fernanda Miraldi Clemente Pessôa[1] · Alessandro Severo Alves de Melo[1] · Arthur Soares Souza Jr.[2] · Luciana Soares de Souza[2] · Bruno Hochhegger[3] · Gláucia Zanetti[4] · Edson Marchiori[4]

Received: 26 April 2016 / Accepted: 6 June 2016 / Published online: 14 June 2016

Abstract The aim of this review was to present the main aspects of pleural diseases seen with conventional and advanced magnetic resonance imaging (MRI) techniques. This modality is considered to be the gold standard for the evaluation of the pleural interface, characterization of complex pleural effusion, and identification of exudate and hemorrhage, as well as in the analysis of superior sulcus tumors, as it enables more accurate staging. The indication for MRI of the thorax in the identification of these conditions is increasing in comparison to computerized tomography, and it can also be used to support the diagnosis of pulmonary illnesses. This literature review describes the morphological and functional aspects of the main benign and malignant pleural diseases assessed with MRI, including mesothelioma, metastasis, lymphoma, fibroma, lipoma, endometriosis, asbestos-related pleural disease, empyema, textiloma, and splenosis.

Keywords Pleural diseases · Magnetic resonance imaging · Mesothelioma · Pleural metastasis

✉ Edson Marchiori
edmarchiori@gmail.com

[1] Universidade Federal Fluminense, Rio De Janeiro, Brazil

[2] Medical School of Rio Preto and Ultra X, São José Do Rio Preto, SP, Brazil

[3] Santa Casa de Porto Alegre, Porto Alegre, Rio Grande do Sul, Brazil

[4] Federal University of Rio de Janeiro, Rua Thomaz Cameron, 438. Valparaiso, Rio De Janeiro, Petrópolis CEP 25685.120, Brazil

Introduction

Imaging investigation of pleural diseases plays a crucial role in decision making regarding therapeutic approaches and prognostic implications resulting from early detection. Magnetic resonance imaging (MRI) of the chest is a non-invasive and nonionizing [1] method that enables the detection of benign and malignant pleural conditions, ranging from pleural effusions to solid tumors, with great accuracy. MRI is superior to ultrasound for the detection and characterization of pleural effusions; it is also superior to computerized tomography (CT), particularly for the characterization of complex pleural effusions (with better visualization of septa in loculated effusions) and the identification of hemorrhage (with increased signal intensity of hemorrhage foci on T1–weighted imaging [WI]). MRI provides more spatial resolution than CT in soft-tissue analysis, which enables better characterization of the pleura–chest wall interface, as well as the study of the great heart vessels, heart, diaphragm, and other critical structures that might be involved. It enables evaluation of the resectability of tumors that have invaded the pleura [2]. The greater sensitivity of MRI with paramagnetic contrast (gadolinium) compared to CT contributes markedly to the superiority of this modality [3, 4].

Initial evaluation with conventional MRI sequences involves the structural characterization of a lesion with T1–WI. These images accurately show anatomical details such as dissociation between the pleural space and expleural fat. T2–WI enables distinction between pleural thickening and nodules on the surface, the detection of leakage, and delineation of tumor margins. Administration of gadolinium following T1–WI enhances the contrast between tissues, increasing the conspicuity of lesional limits and healthy tissue. Some authors have emphasized the

importance of short-tau inversion recovery sequences for the assessment of secondary bone involvement; in these sequences, for example, the low normal signal of the bone marrow is seen as a liquid signal, and cortex line projection secondary to erosion is impaired [2].

Diffusion-weighted sequences and dynamic contrast-enhanced studies (DCSs) enable examination not only of structural damage of the pleura, but also functional impairment [1]. Diffusion-weighted imaging (DWI) is a technique based on the evaluation of Brownian motion of water molecules in the tissue, which can be quantified by the apparent diffusion coefficient (ADC) [5]. Movement is random under normal conditions, but it can be altered and reduced in tissue environments with high cellularity or high protein content, which restrict diffusion to water molecules.

DCSs provide information on perfusion nuances according to pre-set times that include the arrival and clearance of tissue contrast, expressed in a dynamic curve [2, 6–9]. Coolen et al. [1] recently demonstrated that the combined use of DWI and DCS optimizes the detection of malignancy, as DCS increased accuracy from 87.1 to 93.5 % when DWI results were indeterminate.

This state-of-the-art review describes the main clinical applications of MRI of the chest for pleural diseases. The main imaging findings are discussed, with a focus on the characterization of pleural asbestos-related disease, pleural effusion, empyema, and benign neoplasms and malignancies (primary, such as mesothelioma, and secondary, such as direct extension or implants).

Anatomy and Fundamental Pleural Lesions

Pleura is a double membrane composed of mesothelial cells and connective tissue, divided into visceral and parietal, with the latter classified as cervical, mediastinal, costal, and diaphragmatic [10]. An understanding of the topography of the parietal pleura is fundamental for the characterization of diseases, as merely reactive pleural inflammation rarely affects the mediastinal portion [3]. Under normal conditions, a small amount ($\leq$5 mL) of sterile liquid is present between the two pleural leaflets, giving the tissue a tensoadhesive property. Pleural thickness ranges from 2 to 4 mm and is homogenous along the surface, except in the apical region, where it has a slightly irregular aspect at the interface with the lung, which has no appreciable clinical significance. Thus, pleural thickening—continuous or nodular, focal or diffuse, with or without calcification—is the main finding with a high impact on differential diagnosis. Importantly, the insinuation of the parietal pleura in the mediastinum is contiguous with the mediastinal structures, which facilitates the direct extension of expansive processes arising from the pleura and vice versa.

Malignant Disorders

Malignant pleural diseases include malignant mesothelioma and metastasis. Malignant changes tend to exhibit higher signal intensity on T2–WI and more intense enhancement by gadolinium on T1–WI, compared to the adjacent intercostal muscles [3]. The main morphological and functional imaging aspects of these conditions will be discussed separately.

Malignant Mesothelioma

Mesothelioma is a neoplasia derived from mesothelial cells of the peritoneum, pericardium, tunica vaginalis, or pleura. Pleural mesothelioma is the most common form; it accounts for 75 % of cases and is prevalent in the sixth and seventh decades of life [11]. Mesothelioma is commonly associated with exposure to asbestos, with an approximate latency of 35–40 years, but is also related to radiotherapy, tuberculosis, and chronic empyema.

Imaging evaluation is crucial for the detection, characterization, and monitoring of this disease. Its radiological characterization is guided by the pattern of tumor growth, with lobed, circumferential, or concentric pleural thickening, which is usually unilateral. Although CT shows general features that suggest the diagnosis, MRI of the thorax enables superior visualization of anatomical details, due mainly to a higher signal-to-noise ratio, allowing the identification of tumor extension at the transdiaphragmatic level through the chest wall and distinction from concomitant pleural effusion, especially the laminar type (Fig. 1) [11]. Mesothelioma shows intermediate signal intensity on T1–WI, high or moderately high intensity on T2–WI, and moderate enhancement by gadolinium. The use of DWI supports the diagnosis by enabling visualization of the "pointillism signal", representing multiple hyperintense pleural foci and appearing when high (>800) *b* values are used [1]; this signal has a high predictive value for malignancy and is more relevant than circumferential pleural thickening. According to Gill et al. [2], DWI and ADC mapping enable the differentiation of certain mesothelioma subtypes, such as epithelioid and sarcoid; the first subtype is characterized by higher ADC map values than the second subtype, reflecting less restriction of water diffusion.

Metastasis

Metastatic involvement of the pleura comprises mainly the direct extension of bronchogenic carcinoma, followed by implantation from breast cancer and lymphoma involving the ovary or stomach [10]. Undabeitia et al. [12] recently reported a case of glioblastoma multiforme with extraneural

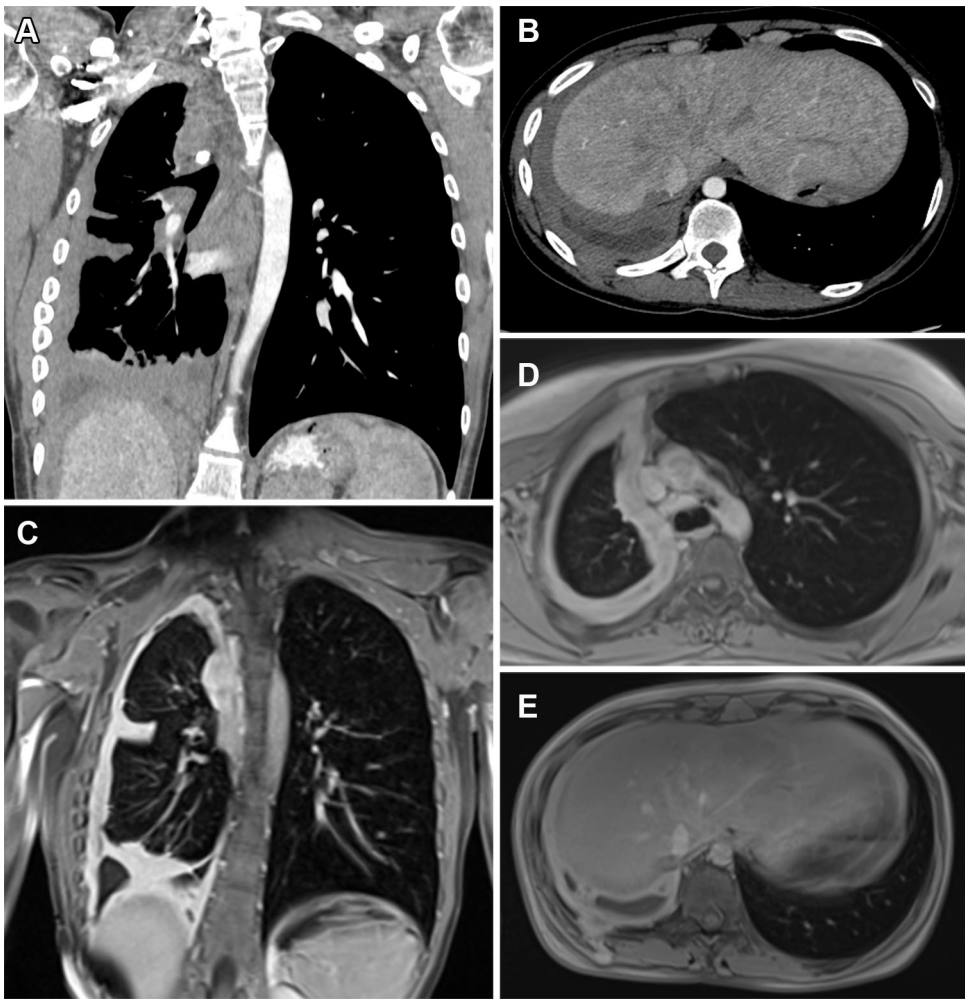

Fig. 1 **a** 53-year-old man with pleural mesothelioma. Coronal (**a**) and axial (**b**) CT images show circumferential and irregular pleural thickening in the right hemithorax, associated with pleural effusion. Coronal (**c**) and axial (**d**, **e**) fat-suppressed T1–WI after paramagnetic contrast administration show intense gadolinium enhancement in the pleural thickening, as well as involvement of mediastinal pleura and fissures with invasion through the posterior chest wall

spread involving the pleura; pleural fluid analysis yielded positive results for glioblastoma multiforme metastasis. The morphostructural aspect of metastasis consists of nodular pleural thickening, which is usually discontinuous along the pleural surface and may also involve the mediastinal pleura; this aspect is common in malignant pleural disease and pleural tuberculosis. The MRI signs of metastasis are related directly to the characteristics of the primary tumor, which tends to have variable signal intensity on T1– and T2–WI (Fig. 2) [2]. As the ADC of the primary tumor is known, this value can be used as a potential marker to identify metastasis [2].

Lymphoma

Hodgkin and non-Hodgkin lymphoma can involve the pleura, resulting in primary or secondary pleural disease [10]. Primary disease is rare, accounting for <0.5 % of all non-Hodgkin lymphoma cases and around 2.5 % of primary chest wall tumors, and it may be a consequence of a chronic complicating pleural effusion [13–15]. **S**econdary pleural lymphoma is very common, occurring in almost 20 % of patients with lymphoma; it may be a result of lymphomatous involvement of the visceral or parietal pleura [13].

In cases of lymphoma, CT and MRI show pleural effusion, pleural nodules, and focal or diffuse and non-circumferential pleural thickening, with homogenous low-contrast enhancement. Multistation adenopathy and marrow involvement are also seen [10]. MRI features include pleural involvement with low signal intensity on T1– and T2–WI, as well as significant restriction of water diffusion in functional analysis. An ADC value of approximately 1.23×10^{-3} mm^2/s may serve as a cut-off value for characterization of these tumors [2].

Benign Disorders

Benign diseases of the pleura include primary benign neoplasms, endometriosis, pleural disease related to asbestos, and tuberculous empyema. The morphofunctional aspects of these diseases are discussed below.

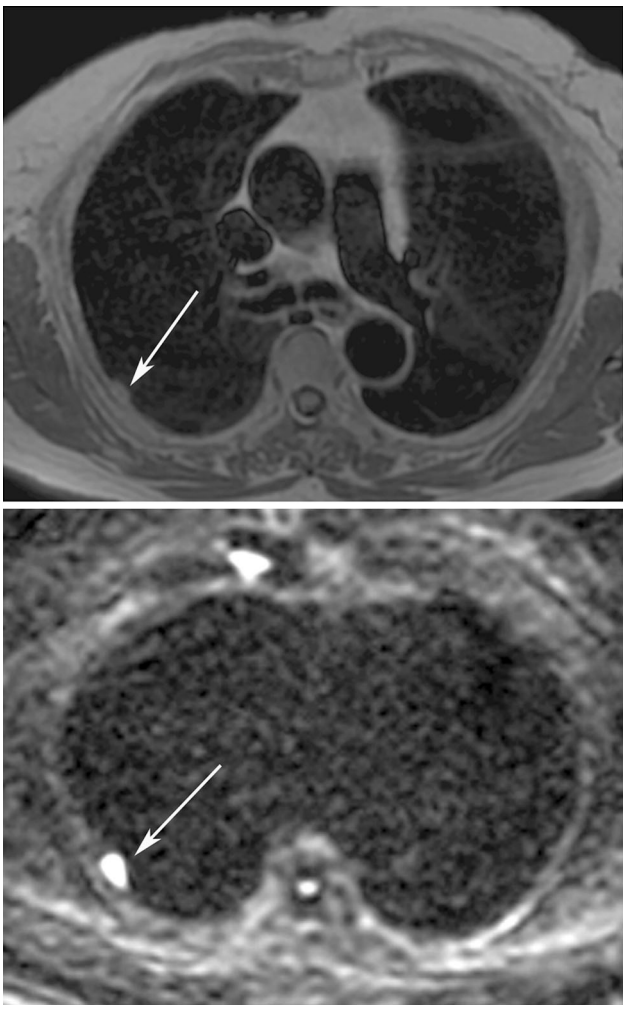

Fig. 2 **a** 71-year-old woman with breast cancer metastasis. Axial T1–WI (**a**) shows a pleural-based nodule (*arrow*) in the right hemithorax with corresponding restriction to water diffusion on DWI (**b**, *arrow*), representing a metastasis

Pleural Fibroma

Pleural fibromas are well-defined heterogeneous masses, usually solitary and pedunculated, with intermediate signal intensity on T1– and T2–WI and high-contrast enhancement (Fig. 3) [14]. About 10 % of these tumors are isointense to soft tissue and 10 % are hyperintense on T1– and T2–WI. Areas of necrosis and myxoid degeneration have high signal intensity on T1– and T2–WI [2]. They are more common in adults and may be associated with localized or general symptoms [1]. According to Santos et al. [3], this tumor can be distinguished from round atelectasis with enough resolution by MRI through detection of the comet tail sign, which reflects the bronchovascular path related to atelectasis parenchyma, with intense and homogeneous post-contrast enhancement. In a recent study, Coolen et al. [1] performed a functional evaluation of these lesions using DWI and ADC mapping, and showed that the identification of the vascular nidus for surgical purposes, using an ADC value of around 1.52×10^{-3} mm^2/s, is possible.

Pleural Lipoma

Pleural lipoma, the most common benign tumor of the pleura, is often an incidental finding [10]. These lesions have hyperintense signals on T1– and T2–WI, with loss of signal in fat-suppression sequences [3]. Functional analysis is generally dispensable, and the differential diagnosis of pleural lipoma is limited due to its rather peculiar morphostructural features.

Endometriosis

Thoracic endometriosis affects the lung parenchyma and pleura and occurs most often between the third and fourth decades of life. The pleural form is commonly manifested as catamenial pneumothorax, generally involving the right side [4, 6, 16]. In conventional MRI sequences, endometriomas can be identified as nodules in the visceral pleural surface, usually associated with pleural effusion or even hydropneumothorax. MRI is very useful in detecting hemoglobin degradation products at the level of the diaphragm or the pleural cavity, which, in the context of endometriomas, is of great value [1]. The implants exhibit marked blood components that may appear hyperintense on T1– and T2–WI, and may be associated with hemorrhagic pleural effusion. In some cases, DWI may be useful to demonstrate diffusion restriction in small endometriomas [16].

Pleural Disease Related to Asbestos

Pleural disease related to asbestos results from cumulative exposure to these inhaled particles, which causes progressive and irreversible changes in the pleura [17]. Pathological events comprise discontinuous pleural thickening in plaques, predominating at the basal regions, associated with calcified plaques that are formed over decades [10]. These changes are not necessarily associated with pleural effusion. Compared to conventional radiography and CT, MRI has great value in the diagnostic evaluation of this entity. In the subclinical stage of the disease, pleural plaques can be less conspicuous, which reduces the sensitivity of these methods. MRI shows superior performance in the detection and characterization of the distribution of these findings in the early stage of the fibrotic process; it can also show round atelectasis not seen in conventional studies, as demonstrated by the series of Bekkelund et al. [17]. The plaques appear hyperintense on T1– and T2–WI and show no post-contrast enhancement. MRI may still show

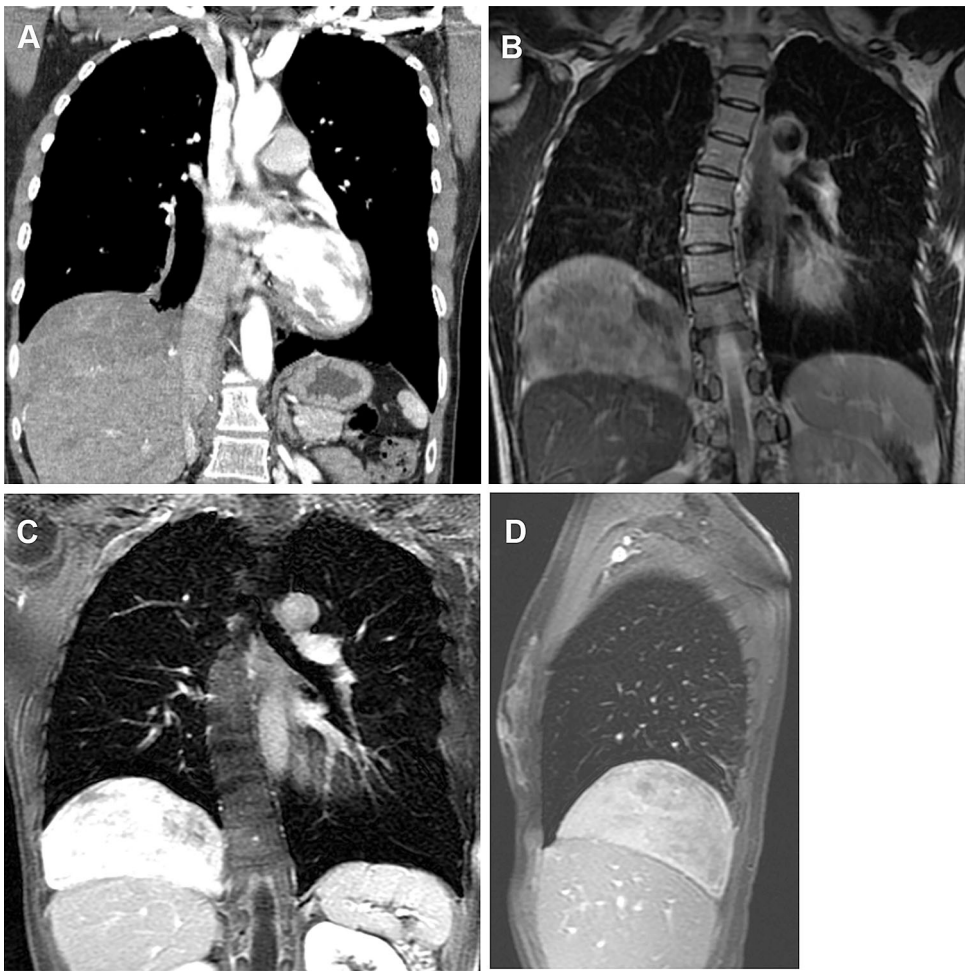

Fig. 3 **a** 42-year-old woman with pleural fibroma.**a**Coronal CT image shows a pedunculated pleural-based and slightly lobulated mass with soft-tissue attenuation and heterogeneous enhancement in the right hemithorax. The margins and the heterogeneous aspect of the lesion are better seen on MRI, as on a coronal T2–WI **b**. Coronal **c**and sagittal **d** fat-suppressed T1–WI after paramagnetic contrast administration show the same lesion with intense gadolinium enhancement

mediastinal lymphadenopathy. The occurrence of mesothelioma is highly prevalent in this population. MRI provides not only morphological information concerning the presence of mesothelioma, but also enables its detection at an early stage in patients with pleural asbestos-related disease. Podobnik et al. [18] showed that benign plaques are hypointense on T2–WI, whereas plaques affected by mesothelioma have a hyperintense appearance, with 100 % correlation between histopathological and imaging findings. Functional assessment by DWI may help to show the absence of restriction in benign plaques. According to Gill et al. [2], the average ADC value for benign plaques is approximately 2.6×10^{-3} mm^2/s, whereas that for mesothelioma plaques is 1.2×10^{-3} mm^2/s.

Pleural Effusion and Empyema

Pleural fluid is typically hypointense on T1–WI and hyperintense on T2–WI, reflecting liquid content. Its appearance may seem to be heterogeneous due to artifacts of fluid motion [1]. Transudates and exudates are related to low signal intensity on T1–WI and high intensity on T2–WI. Exudates may be associated with septa and tend to show hyperintensity on T2–WI, whereas transudates may be isointense compared to muscles [7]. Not infrequently, exudate has septations with delayed enhancement by gadolinium-based contrast [1]. When these findings are associated with a loculated appearance and ≥4 mm pleural thickening, the hypothesis of pleural empyema, especially that of tubercular etiology, assumes important value [10]. In this case, fibrothorax may occur, representing a diffuse fibrotic process along the pleural surface, usually with coarse continuous calcification, which may or may not be associated with pleural effusion at the time of diagnosis. Thickened pleura in tuberculous empyema has hypo or isosignal compared with the muscle signal on T2–WI [1, 3].

MRI also enables the identification of parenchymal or pleural lesions that are not well evidenced on CT in the presence of pleural effusion. Due to differences in signal intensity between tissues and liquid content on MRI,

pleural effusion and pleural-based nodules are better shown on T2–WI and after gadolinium administration (Fig. 4).

Textilomas

"Textiloma" or "gossypiboma" is a term used to describe a mass in the body composed of a cotton matrix, surrounded by a foreign body reaction [19, 20]. Machado et al. [21] showed that the most common site of occurrence of textilomas was the pleural space (14/16 cases; 87.5 %). The pericardial space was involved in only two (12.5 %) cases, in which the lesions were located posteriorly. Some authors have shown that the thoracic site where retained surgical sponges are most commonly found is the pleural space, followed by the pericardial space [20, 22, 23]. Even in studies in which the initiating surgical procedure was heart surgery, the pleural space was the most commonly affected site. When the pericardial space is involved, the mass tends to be located posteriorly [24–26].

On CT, textilomas typically appear as round or oval masses with well-defined and regular contours encapsulated masses with a spongiform pattern and gas bubbles. However, air bubbles may not be as prominent in retained intra-thoracic sponges as they are in retained intra-abdominal sponges [24].

The signal intensity of intra-thoracic textilomas on T1– and T2–WI varies among patients according to MRI findings. MRI typically displays a well-delineated formation with low signal intensity on T1–WI and very high signal intensity on T2–WI. However, low signal intensity of structures on T2–WI has also been reported [27–32].

Splenosis

Thoracic splenosis is a rare condition that involves the autotransplantation of splenic tissue to abnormal locations, usually after combined splenic and diaphragmatic injury, which can occur 20 years before the diagnosis. The basic pathogenesis of splenosis involves a splenic implant onto a serosal surface with the aid of adult spleen reticulum cells, which retain the potential for differentiation into various splenic elements. This condition may occur on the parietal or visceral pleura, appearing as multiple or solitary pleural-based nodules $\leq$3 cm in diameter (some may be larger and form masses) [32, 33].

On CT, thoracic splenosis appears with attenuation and contrast enhancement similar to that of the normal spleen, whereas on MRI it is characterized by a lobulated pleural mass and well-circumscribed pleural-based nodules with intermediate signal intensity on T1– and T2–WI, showing restricted diffusion to water as does the main organ (Fig. 5) [33]. The absence of the spleen in the left upper quadrant is a notable associated finding [32].

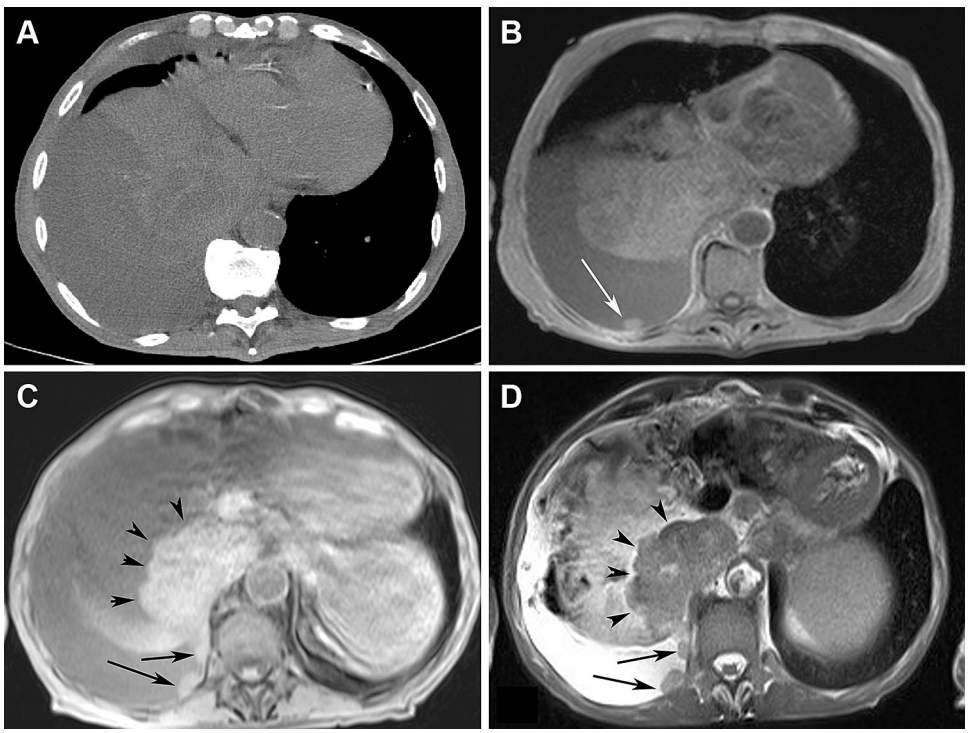

Fig. 4 **a** 67-year-old man with bronchogenic carcinoma, pleural effusion, and pleural metastasis. **a** Axial CT image shows pleural effusion in the right hemithorax. **b** Axial fat-suppressed T1–WI shows a pleural-based nodule (*white arrow*) with intermediate signal intensity and pleural effusion. **c** Axial fat-suppressed T1–WI after paramagnetic contrast administration shows a lung tumor (*arrow heads*) and pleural nodules (*black arrows*) with contrast enhancement. **d** The referred mass and nodules exhibit high signal intensity on T2-WI, representing pleural metastasis (*black arrow*)

Table 1 MR characteristics of pleural diseases

Pleural diseases	T1 signal intensity	T2 signal intensity	Contrast enhancement	Restriction to water diffusion
Malignant Mesothelioma	Low	High	+++	Yes
Metastasis	Low	Low/High	Variable	Yes
Lymphoma	Low	Low	++	Yes
Fibroma	Low	Low	++	Variable
Lipoma	High	Intermediate/High	No	No
Endometriosis	High	High	+	No
Pleural disease related to asbestos	Low	Low	No	No
Pleural effusion and empyema	Low	High	+++	Yes
Textilomas	Low	High	No	No
Splenosis	Intermediate	Intermediate	+	Yes

Table 2 Morphological features and associated findings in pleural diseases

Pleural diseases	Morphological features	Associated findings
Malignant mesothelioma	Circumferential and nodular pleural thickening	Asbestos exposure
		Recurrent pleural effusion
	Usually unilateral	
	Possible extrapleural fat invasion	
Metastasis	Irregular or nodular pleural thickening	Primary malignant disease
	Focal or diffuse	Recurrent pleural effusion
	Involves mediastinal pleura	
Lymphoma	Non-circumferential and nodular pleural thickening	Multistation adenopathy and marrow involvement
	Focal or diffuse	
	Involves mediastinal pleura	
Fibroma	Well-defined heterogeneous mass	
	Usually solitary and pedunculated	
Lipoma	Well-defined homogeneous mass	Accidental imaging finding
	Usually solitary	
	Fat density	
Endometriosis	Nodules in the visceral pleural surface.	Catamenial pneumothorax
		Hemorrhage pleural effusion
Pleural disease related to asbestos	Multifocal pleural thickening with calcified plaques	Pleural effusion
		Round atelectasis
	Involves diaphragmatic pleura	
	Extrapleural fat preservation	
Pleural effusion and empyema	Pleural thickening	Clinical and occasional pulmonary imaging findings of infectious disease
	"Split pleura sign"	
	Loculations	
	Internal septations	
Textilomas	Well-defined encapsulated mass in pleural space	Previous cardiothoracic surgery
	Spongiform pattern and gas bubbles	
Splenosis	Well-circumscribed pleural-based nodules	Previous splenic and diaphragmatic injury

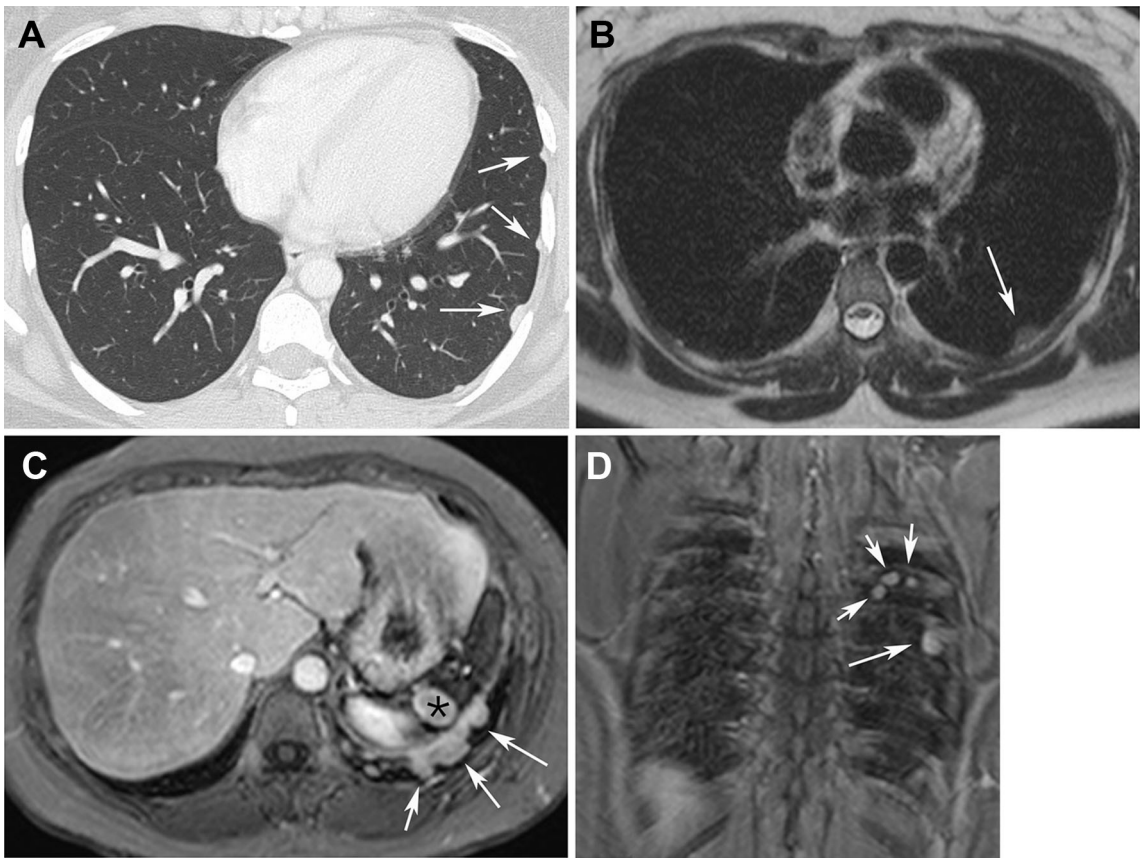

Fig. 5 **a** 32-year-old woman with pleural splenosis. **a** Axial CT image shows well-circumscribed pleural-based nodules (*white arrows*) in the left hemithorax. The same nodules are observed on MRI with intermediate signal intensity on axial T2–WI **b** and contrast enhancement similar to that of residual spleen parenchyma (*black asterisk*), as can be seen on axial **c** and coronal **d** fat-suppressed T1–WI after paramagnetic contrast administration

Conclusion

The most suggestive findings of malignant pleural disease are the involvement of mediastinal pleura, circumferential pleural thickening, nodularity, pleural irregularities, and infiltration of the chest wall or diaphragm. Otherwise, tumor-like conditions of the pleura, such as pleural endometriosis, pleural splenosis, pleural pseudotumors, and pleural plaques, are important to consider in the differential diagnosis of neoplastic lesions. The recognition of certain imaging patterns has been supported by MRI, especially in the evaluation of the chest wall and pleuropulmonary interface [34, 35] (Tables 1 and 2). In addition to morphological changes, the MRI signal and post-contrast enhancement characteristics can increase the specificity of these patterns compared with CT. MRI is a superior method for the evaluation of invasion of the chest wall and diaphragm, and is therefore the gold standard for evaluation of the resectability of pleural lesions. Some advantages of CT persist, however, such as greater sensitivity in the detection of pleural calcifications, suggestive of benignity, the identification of bone destruction by a malignant lesion, and the guiding of pleural biopsy.

Compliance with Ethical Standards

Conflict of Interest None.

References

1. Coolen J, Verschakelen J, de Wever W (2015) MRI of pleural disease. Curr Opin Pulm Med 21:399–406
2. Gill RR, Patz S, Muradyan I et al (2015) Novel MR imaging applications for pleural evaluation. Magn Reson Imaging Clin N Am 23:179–195
3. Santos MK, Júnior JE, Mauad FM et al (2011) Magnetic resonance imaging of the chest: current and new applications, with an emphasis on pulmonology. J Bras Pneumol 37:242–258
4. Semelka RC, Cem Balci N, Wilber KP et al (2000) Breath-hold 3D gradient-echo MR imaging of the lung parenchyma: evaluation of reproducibility of image quality in normals and preliminary observations in patients with disease. J Magn Reson Imaging 11:195–200
5. Coolen J, De Keyzer F, Nafteux P et al (2012) Malignant pleural disease: diagnosis by using diffusion-weighted and dynamic

contrast-enhanced MR imaging-initial experience. Radiol 263:884–892
6. Mehndiratta A, Knopp MV, Zechmann CM et al (2009) Comparison of diagnostic quality and accuracy in color-coded versus grayscale DCE-MR imaging display. Int J CARS 4:457–462
7. Inan N, Arslan A, Akansel G et al (2009) Diffusion-weighted MRI in the characterization of pleural effusions. Diagn Interv Radiol 15:13–18
8. Luna A, Sánchez-Gonzalez J, Caro P (2011) Diffusion-weighted imaging of the chest. Magn Reson Imaging Clin N Am 19:69–94
9. Giesel FL, Choyke PL, Mehndiratta A et al (2008) Pharmacokinetic analysis of malignant pleural mesothelioma: initial results of tumor microcirculation and its correlation to microvessel density (CD-34). Acad Radiol 15:563–570
10. Sureka B, Thukral BB, Mittal MK et al (2013) Radiological review of pleural tumors. Indian J Radiol Imaging 23:313–320
11. Armato SG III, Labby ZE, Coolen J et al (2013) Imaging in pleural mesothelioma: a review of the 11th international conference of the international mesothelioma interest Group. Lung Cancer 82:190–196
12. Undabeitia J, Castle M, Arrazola M et al (2015) Multiple extraneural metastasis of glioblastoma multiforme. An Sist Sanit Navar 38:157–161
13. Dynes MC, White EM, Fry WA et al (1992) Imaging manifestations of pleural tumors. Radiographics 12:1191–1201
14. Giardino A, O'Regan KN, Hargreaves J et al (2011) Primary pleural lymphoma without associated pyothorax. J Clin Oncol 29:413–415
15. Alexandrakis MG, Passam FH, Kyriakou DS et al (2004) Pleural effusions in hematologic malignancies. Chest 125:1546–1555
16. Rosado-de-Christenson ML, Abbott GF, McAdams HP et al (2003) Localized fibrous tumors of the pleura. Radiographics 23:759–783
17. Marchiori E, Zanetti G, Rodrigues RS et al (2012) Pleural endometriosis: findings on magnetic resonance imaging. J Bras Pneumol 38:797–802
18. Bekkelund SI, Aasebo U, Pierre-Jerome C et al (1998) Magnetic resonance imaging of the thorax in the evaluation of asbestosis. Eur Respir J 11:194–197
19. Martins MC, Amaral RP, Andrade CS et al (2009) Características de imagem na ressonância magnética de gossipiboma intracraniano: relato de caso e revisão da literatura. Radiol Bras. 42:407–409
20. Poncelet AJ, Watremez C, Tack D et al (2005) Paracardiac opacity following inferior and middlelobe resection for bronchogenic carcinoma: unsuspected diagnosis. Chest 128:439–441
21. Machado DM, Zanetti G, Neto CA et al (2014) Thoracic textilomas: CT findings. J Bras Pneumol 40:535–542
22. Vayre F, Richard P, Ollivier JP (1999) Intrathoracic gossypiboma: magnetic resonance features. Int J Cardiol 70:199–200
23. Coşkun M, Boyvat F, Ağildere AM (1999) CT features of a pericardial gossypiboma. Eur Radiol 9:728–730
24. Nobre LF, Marchiori E, May F et al (2010) Thoracic textilomas after myocardial revascularisation: typical CT Findings. Br J Radiol 83:4–7
25. Suwatanapongched T, Boonkasem S, Sathianpitayakul E et al (2005) Intrathoracic gossypiboma: radiographic and CT findings. Br J Radiol 78:851–853
26. Scott WW, Beall DP, Wheeler PS (1991) The retained intrapericardial sponge: value of the lateral chest radiograph. AJR Am J Roentgenol 171:595–597
27. Kuwashima S, Yamato M, Fujioka M et al (1993) MR findings of surgically retained sponges and towels: report of two cases. Radiat Med 11:98–101
28. Sugimura H, Tamura S, Kakitsubata Y et al (1992) Magnetic resonance imaging of retained surgical sponges.Case report. Clin Imaging 16:259–262
29. Roumen RM, Weerdenburg HP (1998) MR features of a 24-year-old gos-sypiboma.a case report. Acta Radiol 39:176–178
30. Buy JN, Hubert C, Ghossain MA et al (1989) Computed tomography of retained abdominal sponges and towels. Gastrointest Radiol 14:41–45
31. Durmaz DY, Yilmaz BK, Yildiz O et al (2014) A Rare Cause of Chronic Cough: intrathoracic Gossypiboma. Iran J Radiol 11:e13933
32. Mançano AD, Zanetti G, Duarte BC et al (2012) Thoracic splenosis after thoracoabdominal trauma presentingas pleural nodules. Lung 190:699–701
33. Marchiori E, Rodrigues RS, Reis MCM et al (2014) Pleural nodules in a patient with a colonic tumour. Thorax 69:395
34. Podobnik J, Kocijancic I, Kovac V et al (2010) 3T MRI in evaluation of asbestosis-related thoracic diseases-preliminary results. Radiol Oncol 44:92–96
35. de Paula MC, Escuissato DL, Belém LC et al (2015) Pleural tumorlike conditions: nodules and masses beyond mesotheliomas and metastasis. Respir Med 109:1235–1243